JOURNAL OF BIOMEDICAL OPTICS 3(2), 212–220 (APRIL 1998)

LIGHT SCATTERING MULTIPOLE SOLUTION FOR A CELL

Gorden Videen[†] and Dat Ngo[‡]
[†]Army Research Laboratory AMSRL-IS-EE, Adelphi, Maryland 20783-1197; [‡]NgoCo, 5934 Roosevelt Boulevard, Philadelphia, Pennsylvania 19149

(Paper JBO-165 received Jul. 28, 1997; revised manuscript received Nov. 4, 1997; accepted for publication Nov. 21, 1997.)

ABSTRACT

We derive a multipole scattering solution for a system resembling a simple cell. In the model, a spherical cytoplasm is surrounded by a concentric cell membrane. Contained within the cytoplasm is a nonconcentric spherical nucleus. Because of the nature of the (multipole expansion) solution, numerical results can be acquired quite rapidly. We show that the resulting scatter is very sensitive to the system geometry and optical properties. Such a solution may also be used to calculate the scatter from fluorescing molecules located within the cell. © *1998 Society of Photo-Optical Instrumentation Engineers.* [S1083-3668(98)01002-8]

Keywords scattering; cell; polarization.

1 INTRODUCTION

Light scattering is a sensitive tool which can be used to determine the geometry and composition of particle systems. Such a valuable tool has been used in the laboratory to characterize biological systems from bacteria to red blood cells.[1–11] The polarization state of the scattered light expressed by the light scattering Mueller matrix has been shown to be especially sensitive to small changes in the system.[5–8]

Modeling the scattering from complex cellular systems is difficult due to their complex cellular structure, and as a result very few programs have been developed in this field. One approach has been to take advantage of the cell's relatively small refractive index within the host medium and to use the anomalous diffraction approximation.[9,10] Another approach has been to apply the finite-difference time-domain technique to cells.[12,13] Although both techniques have proven valuable, they are both limited. The anomalous diffraction approximation does not accurately predict the backscatter from systems. It is in this backscatter region that polarization techniques have been shown to be especially sensitive to small changes in the system geometry and chemistry. Although the finite-difference time-domain technique can model virtually any system, it is extremely computer intensive.

In this paper we develop a model which can be used to approximate the scatter from a cellular system. This technique uses a multipole expansion of the fields internal and external to the cell. The cellular system is shown in Figure 1. It is composed of a spherical cytoplasm surrounded by a spherical cell membrane. Contained within the cytoplasm is a spherical nucleus. The nucleus can be placed at any location within the cytoplasm. Although this model is also severely limited, since the components of the cell are restricted to being spherical, it does have some advantages. First, calculations are very rapid, and second, the calculations are exact. This model can be used to examine the effects of certain system parameters, such as the cell membrane composition or thickness, the nucleus size and position, or the inclusion of organelles within the cytoplasm or changes in the cytoplasm chemistry. The derivation is similar to that of previous works[14,15] in which we examined the scatter from a randomly placed particle within a spherical host. In the present work, a concentric outer layer is added to the host (cytoplasm) to represent a cell membrane. We will show in the results section that the inclusion of this concentric cell membrane surrounding the cytoplasm can affect the polarization state of the scattered light, especially in the backscatter region.

Finally, we note that since this is a complete solution, both the scattered and internal fields are known for the system. Using reciprocity and the solution for the internal fields, the scattered fields from a fluorescing molecule located at any position within the cell can be calculated.[16]

2 SOLUTION

The geometry of the scattering system is shown in Figure 1. A spherical cytoplasm of radius a_1 and complex refractive index m_1 is centered on the x_1, y_1, z_1 coordinate system. An outer, concentric cell membrane having outer radius a_3 and complex refractive index m_3 is also centered on the x_1, y_1, z_1 coordinate system such that $a_1 < a_3$. A spherical

Address all correspondence to Gorden Videen. Tel: (301) 394-1871; Fax: (301) 394-4797; E-mail: videen@atm.dal.ca

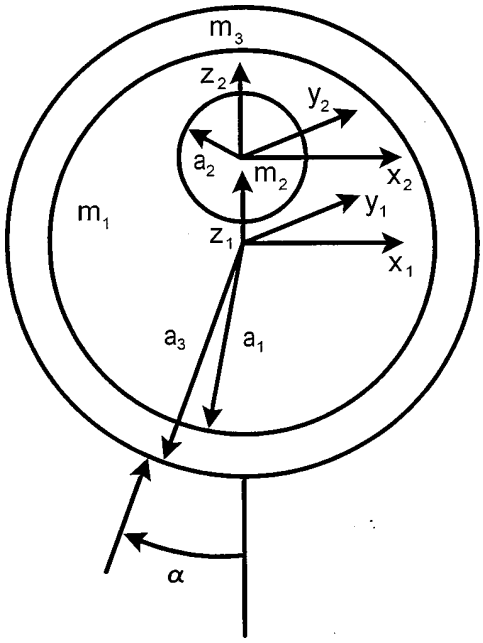

Fig. 1 Geometry of the cell.

nucleus of radius a_2 and complex refractive index m_2 is centered on the x_2, y_2, z_2 coordinate system at a position $x_1=0$, $y_1=0$, $z_1=d$ such that $a_1-a_2>|d|$. In order for the scattering geometry to be completely general, the wave vector of the incident radiation is oriented at angle α with respect to the z_1 axis. The wavelength and wave vector of the plane wave in the nonabsorbing, nonmagnetic incident medium are λ and k, respectively. The complex wave vector in media of refractive index m_j is k_j. To simplify the equations, we make the permeability of the spheres and the surrounding media the same.

The scattering solution can be found by simultaneously satisfying the boundary conditions at each interface. We consider the fields incident on each cell component separately. These fields are expanded in terms of the vector spherical harmonics which have the following form in this derivation:

$$M_{nm,j}^{(\rho)}=\hat{\theta}_j\left[\frac{im}{\sin\theta_j}z_n^{(\rho)}(kr_j)\tilde{P}_n^m(\cos\theta_j)e^{im\varphi_j}\right]-\hat{\varphi}_j\left[z_n^{(\rho)}(kr_j)\frac{d}{d\theta_j}\tilde{P}_n^m(\cos\theta_j)e^{im\varphi_j}\right], \quad (1)$$

$$N_{nm,j}^{(\rho)}=\hat{r}_j\left[\frac{1}{kr_j}z_n^{(\rho)}(kr_j)n(n+1)\tilde{P}_n^m(\cos\theta_j)e^{im\varphi_j}\right]+\hat{\theta}_j\left[\frac{1}{kr_j}\frac{d}{dr_j}[r_jz_n^{(\rho)}(kr_j)]\frac{d}{d\theta_j}\tilde{P}_n^m(\cos\theta_j)e^{im\varphi_j}\right]+\hat{\varphi}_j\left[\frac{1}{kr_j}\frac{d}{dr_j}[r_jz_n^{(\rho)}(kr_j)]\times\frac{im}{\sin\theta_j}\tilde{P}_n^m(\cos\theta_j)e^{im\varphi_j}\right], \quad (2)$$

where the index j corresponds to the coordinate system used ($j=1,2$) and $z_n^{(\rho)}(kr_j)$ are the spherical Bessel functions of the first, second, third, or fourth kind ($\rho=1, 2, 3, 4$), and

$$\tilde{P}_n^m(\cos\theta_j)=\sqrt{\frac{(2n+1)(n-m)!}{2(n+m)!}}P_n^m(\cos\theta_j), \quad (3)$$

where $P_n^m(\cos\theta_j)$ are the associated Legendre polynomials. We assume a time dependence of $\exp(-i\omega t)$.

2.1 OUTER CELL-MEMBRANE INTERFACE

We first examine the fields which strike the outermost cell-membrane interface ($r_1=a_3$). We consider an arbitrary field incident on the system which can be expanded using the spherical Bessel functions of the first kind, $j_n(kr_1)$:

$$E_{\text{inc}}^1=\sum_{n=0}^{\infty}\sum_{m=-n}^{n}a_{nm}M_{nm,1}^{(1)}+b_{nm}N_{nm,1}^{(1)}. \quad (4)$$

Similarly, the scattered electric field may be expanded using the spherical Bessel functions of the third kind, $h_n^{(1)}(kr_1)$:

$$E_{\text{sca}}^1=\sum_{n=0}^{\infty}\sum_{m=-n}^{n}c_{nm}M_{nm,1}^{(3)}+d_{nm}N_{nm,1}^{(3)}. \quad (5)$$

The fields inside the cell membrane may be expanded into incoming and outgoing spherical waves using spherical Bessel functions of the fourth kind $h_n^{(2)}(k_1r_1)$ and third kind $h_n^{(1)}(k_1r_1)$:

$$E_{\text{con}}^1=\sum_{n=0}^{\infty}\sum_{m=-n}^{n}i_{nm}M_{nm,1}^{(3)}+j_{nm}N_{nm,1}^{(3)}+k_{nm}M_{nm,1}^{(4)}+l_{nm}N_{nm,1}^{(4)}. \quad (6)$$

The application of boundary conditions at the outer cell-membrane interface for the above three equations yields two sets of equations:

$$a_{nm}k_3\psi_n(ka_3)+c_{nm}k_3\xi_n^{(1)}(ka_3)=i_{nm}k\xi_n^{(1)}(k_3a_3)+k_{nm}k\xi_n^{(2)}(k_3a_3), \quad (7)$$

$$a_{nm}\psi_n'(ka_3)+c_{nm}\xi_n'^{(1)}(ka_3)=i_{nm}\xi_n'^{(1)}(k_3a_3)+k_{nm}\xi_n'^{(2)}(k_3a_3), \quad (8)$$

$$b_{nm}\psi_n(ka_3)+d_{nm}\xi_n^{(1)}(ka_3)=j_{nm}\xi_n^{(1)}(k_3a_3)+l_{nm}\xi_n^{(2)}(k_3a_3), \quad (9)$$

$$b_{nm}k_3\psi_n'(ka_3)+d_{nm}k_3\xi_n'^{(1)}(ka_3)=j_{nm}k\xi_n'^{(1)}(k_3a_3)+l_{nm}k\xi_n'^{(2)}(k_3a_3), \quad (10)$$

where $\psi_n(r)$ and $\xi_n^{(q)}(r)$ $(q=1,2)$ are the Riccati–Bessel functions defined by

$$\psi_n(r)=rj_n(r) \quad \text{and} \quad \xi_n^{(q)}(r)=rh_n^{(q)}(r), \tag{11}$$

and the primes denote derivatives with respect to the argument.

2.2 CYTOPLASM-CELL-MEMBRANE INTERFACE

We now examine the fields which strike the cytoplasm-cell-membrane interface ($r_1=a_1$). The fields in the region $|d|<r_1<a_1$ may be expanded into incoming and outgoing spherical waves using spherical Bessel functions of the fourth kind, $h_n^{(2)}(kr_1)$, and third kind, $h_n^{(1)}(kr_1)$:

$$E_{\text{sph}}^1=\sum_{n=0}^{\infty}\sum_{m=-n}^{n} e_{nm}M_{nm,1}^{(3)}+f_{nm}N_{nm,1}^{(3)}+g_{nm}M_{nm,1}^{(4)} +h_{nm}N_{nm,1}^{(4)}. \tag{12}$$

The application of boundary conditions at the cytoplasm-cell-membrane interface yields two sets of equations:

$$i_{nm}k_1\xi_n^{(1)}(k_3a_1)+k_{nm}k_1\xi_n^{(2)}(k_3a_1) =e_{nm}k_3\xi_n^{(1)}(k_1a_1)+g_{nm}k_3\xi_n^{(2)}(k_1a_1), \tag{13}$$

$$i_{nm}\xi_n'^{(1)}(k_3a_1)+k_{nm}\xi_n'^{(2)}(k_3a_1) =e_{nm}\xi_n'^{(1)}(k_1a_1)+g_{nm}\xi_n'^{(2)}(k_1a_1), \tag{14}$$

$$j_{nm}\xi_n^{(1)}(k_3a_1)+l_{nm}\xi_n^{(2)}(k_3a_1) =f_{nm}\xi_n^{(1)}(k_1a_1)+h_{nm}\xi_n^{(2)}(k_1a_1), \tag{15}$$

$$j_{nm}k_1\xi_n'^{(1)}(k_3a_1)+l_{nm}k_1\xi_n'^{(2)}(k_3a_1) =f_{nm}k_3\xi_n'^{(1)}(k_1a_1)+h_{nm}k_3\xi_n'^{(2)}(k_1a_1). \tag{16}$$

Since our primary concern is with the scattered fields, we can write the scattered and internal field coefficients directly in terms of the cytoplasm internal field coefficients.

$$a_{nm}A_n^{(J)}+c_{nm}C_n^{(J)}=e_{nm}E_n^{(J)}+g_{nm}G_n^{(J)}, \tag{17}$$

$$b_{nm}B_n^{(J)}+d_{nm}D_n^{(J)}=f_{nm}F_n^{(J)}+h_{nm}H_n^{(J)}, \tag{18}$$

where $J=1$ or 2. The coefficients can be found from Eqs. (7) to (10) and (13) to (16), and by applying the Wronskian formula for Riccati–Bessel functions[17]

$$W[\xi_n^{(1)}(z),\xi_n^{(2)}(z)]=-2i, \tag{19}$$

the following expressions for these coefficients may be derived:

$$A_n^{(J)}=k_1k_3\psi_n(ka_3)\xi_n'^{(J)}(k_3a_3)-kk_1\psi_n'(ka_3)\xi_n^{(J)}(k_3a_3), \tag{20}$$

$$B_n^{(J)}=kk_1\psi_n(ka_3)\xi_n'^{(J)}(k_3a_3)-k_1k_3\psi_n'(ka_3)\xi_n^{(J)}(k_3a_3), \tag{21}$$

$$C_n^{(J)}k_1k_3\xi_n^{(1)}(ka_3)\xi_n'^{(J)}(k_3a_3)-kk_1\xi_n'^{(1)}(ka_3)\xi_n^{(J)}(k_3a_3), \tag{22}$$

$$D_n^{(J)}=kk_1\xi_n^{(1)}(ka_3)\xi_n'^{(J)}(k_3a_3)-k_1k_3\xi_n'^{(1)}(ka_3) \times\xi_n^{(J)}(k_3a_3), \tag{23}$$

$$E_n^{(J)}=kk_3\xi_n^{(1)}(k_1a_1)\xi_n'^{(J)}(k_3a_1)-kk_1\xi_n'^{(1)}(k_1a_1) \times\xi_n^{(J)}(k_3a_1), \tag{24}$$

$$F_n^{(J)}=kk_1\xi_n^{(1)}(k_1a_1)\xi_n'^{(J)}(k_3a_1)-kk_3\xi_n'^{(1)}(k_1a_1) \times\xi_n^{(J)}(k_3a_1), \tag{25}$$

$$G_n^{(J)}=kk_3\xi_n^{(2)}(k_1a_1)\xi_n'^{(J)}(k_3a_1)-kk_1\xi_n'^{(2)}(k_1a_1) \times\xi_n^{(J)}(k_3a_1), \tag{26}$$

$$H_n^{(J)}=kk_1\xi_n^{(2)}(k_1a_1)\xi_n'^{(J)}(k_3a_1)-kk_3\xi_n'^{(2)}(k_1a_1) \times\xi_n^{(J)}(k_3a_1). \tag{27}$$

2.3 CYTOPLASM-NUCLEUS INTERFACE

We now examine the fields which strike the cytoplasm-nucleus interface. We will examine these fields in the x_2, y_2, z_2 coordinate system $(j=2)$. The fields inside the nucleus may be expressed by the spherical Bessel functions of the first kind $j_n(k_2r_2)$:

$$E_{\text{int}}^2=\sum_{n=0}^{\infty}\sum_{m=-n}^{n} p_{nm}M_{nm,2}^{(1)}+q_{nm}N_{nm,2}^{(1)}. \tag{28}$$

The fields in the cytoplasm may be expressed into incoming and outgoing spherical waves using spherical Bessel functions of the fourth kind $h_n^{(2)}(k_1r_2)$ and third kind $h_n^{(1)}(k_1r_2)$:

$$E_{\text{ext}}^2=\sum_{n=0}^{\infty}\sum_{m=-n}^{n} r_{nm}M_{nm,2}^{(3)}+s_{nm}N_{nm,2}^{(3)}+t_{nm}M_{nm,2}^{(4)} +u_{nm}N_{nm,2}^{(4)}. \tag{29}$$

Applying boundary conditions at the inclusion sphere interface yields two sets of equations:

$$p_{nm}k_1\psi_n(k_2a_2)=r_{nm}k_2\xi_n^{(1)}(k_1a_2)+t_{nm}k_2\xi_n^{(2)}(k_1a_2), \tag{30}$$

$$p_{nm}\psi_n'(k_2a_2)=r_{nm}\xi_n'^{(1)}(k_1a_2)+t_{nm}\xi_n'^{(2)}(k_1a_2), \tag{31}$$

$$q_{nm}\psi_n(k_2a_2)=s_{nm}\xi_n^{(1)}(k_1a_2)+u_{nm}\xi_n^{(2)}(k_1a_2), \tag{32}$$

$$q_{nm}k_1\psi_n'(k_2a_2)=s_{nm}k_2\xi_n'^{(1)}(k_1a_2)+u_{nm}k_2\xi_n'^{(2)}(k_1a_2). \tag{33}$$

We can eliminate the nucleus field coefficients (p_{nm} and q_{nm}) to find relationships for the cytoplasm field coefficients. After a little bit of algebra, we have:

$$r_{nm}=t_{nm}\frac{k_1\xi_n'^{(2)}(k_1a_2)\psi_n(k_2a_2)-k_2\xi_n^{(2)}(k_1a_2)\psi_n'(k_2a_2)}{k_2\xi_n^{(1)}(k_1a_2)\psi_n'(k_2a_2)-k_1\xi_n'^{(1)}(k_1a_2)\psi_n(k_2a_2)}$$

$$=Q_n^r t_{nm}, \tag{34}$$

$$s_{nm}=u_{nm}\frac{k_2\xi_n'^{(2)}(k_1a_2)\psi_n(k_2a_2)-k_1\xi_n^{(2)}(k_1a_2)\psi_n'(k_2a_2)}{k_1\xi_n^{(1)}(k_1a_2)\psi_n'(k_2a_2)-k_2\xi_n'^{(1)}(k_1a_2)\psi_n(k_2a_2)}$$

$$=Q_n^s u_{nm}. \tag{35}$$

The coefficients (Q_n^r and Q_n^s) are similar to the Mie scattering coefficients.[18]

2.4 FIELDS IN THE CYTOPLASM

The fields interior to the cytoplasm are expressed by Eqs. (7)–(10), while the fields exterior to the nucleus are expressed by Eqs. (34) and (35). These fields are identical. We can equate these fields and express the coefficients e_{nm}, f_{nm}, g_{nm}, and h_{nm} in terms of the coefficients r_{nm}, s_{nm}, t_{nm}, and u_{nm} using the translation addition theorem. For a translation along the z axis with no rotation, the vector spherical harmonics are related by

$$M_{nm,2}^{(q)}=\sum_{n'=0}^{\infty}A_{n'}^{(n,m)}M_{n'm,1}^{(q)}+B_{n'}^{(n,m)}N_{n'm,1}^{(q)}, \tag{36}$$

$$N_{nm,2}^{(q)}=\sum_{n'=0}^{\infty}B_{n'}^{(n,m)}M_{n'm,1}^{(q)}+A_{n'}^{(n,m)}N_{n'm,1}^{(q)}, \tag{37}$$

where q denotes the order of the spherical Bessel functions ($q=3,4$). This relationship is valid in the region where $r>|d|$. Explicit expressions by which these coefficients can be calculated are provided in Appendix A. Substituting Eqs. (36) and (37) into Eq. (29) yields

$$e_{nm}=\sum_{n'=0}^{\infty}r_{n'm}A_n^{(n',m)}+s_{n'm}B_n^{(n',m)}, \tag{38}$$

$$f_{nm}=\sum_{n'=0}^{\infty}s_{n'm}A_n^{(n',m)}+r_{n'm}B_n^{(n',m)}, \tag{39}$$

$$g_{nm}=\sum_{n'=0}^{\infty}t_{n'm}A_n^{(n',m)}+u_{n'm}B_n^{(n',m)}, \tag{40}$$

and

$$h_{nm}=\sum_{n'=0}^{\infty}u_{n'm}A_n^{(n',m)}+t_{n'm}B_n^{(n',m)}. \tag{41}$$

Substituting Eqs. (38) and (41) into Eqs. (17) and (18) yields

$$a_{nm}A_n^{(J)}+c_{nm}C_n^{(J)}=\sum_{n'=0}^{\infty}t_{n'm}A_n^{(n',m)}[G_n^{(J)}+Q_{n'}^r,E_n^{(J)}]+u_{n'm}B_n^{(n',m)}[G_n^{(J)}+Q_{n'}^s,E_n^{(J)}] \tag{42}$$

and

$$b_{nm}B_n^{(J)}+d_{nm}D_n^{(J)}=\sum_{n'=0}^{\infty}t_{n'm}B_n^{(n',m)}[H_n^{(J)}+Q_{n'}^r,F_n^{(J)}]+u_{n'm}A_n^{(n',m)}[H_n^{(J)}+Q_{n'}^s,F_n^{(J)}]. \tag{43}$$

The exterior field coefficients of the nucleus, t_{nm} and u_{nm}, may be calculated by eliminating the scattering coefficients, c_{nm} and d_{nm}, in Eqs. (42) and (43):

$$a_{nm}\alpha_n=\sum_{n'=0}^{\infty}t_{n'm}T_{n'}^{(n,m,1)}+u_{n'm}U_{n'}^{(n,m,1)}, \tag{44}$$

$$b_{nm}\beta_n=\sum_{n'=0}^{\infty}t_{n'm}T_{n'}^{(n,m,2)}+u_{n'm}U_{n'}^{(n,m,2)}, \tag{45}$$

where

$$\alpha_n=A_n^{(1)}C_n^{(2)}-A_n^{(2)}C_n^{(1)}, \tag{46}$$

$$\beta_n=B_n^{(1)}D_n^{(2)}-B_n^{(2)}D_n^{(1)}, \tag{47}$$

$$T_{n'}^{(n,m,1)}=A_n^{(n',m)}\{C_n^{(2)}[G_n^{(1)}+Q_{n'}^r,E_n^{(1)}]-C_n^{(1)}[G_n^{(2)}+Q_{n'}^r,E_n^{(2)}]\}, \tag{48}$$

$$T_{n'}^{(n,m,2)}=B_n^{(n',m)}\{D_n^{(2)}[H_n^{(1)}+Q_{n'}^r,F_n^{(1)}]-D_n^{(1)}[H_n^{(2)}+Q_{n'}^r,F_n^{(2)}]\}, \tag{49}$$

$$U_{n'}^{(n,m,1)}=B_n^{(n',m)}\{C_n^{(2)}[G_n^{(1)}+Q_{n'}^s,E_n^{(1)}]-C_n^{(1)}[G_n^{(2)}+Q_{n'}^s,E_n^{(2)}]\}, \tag{50}$$

$$U_{n'}^{(n,m,2)} = A_n^{(n',m)}\{D_n^{(2)}[H_n^{(1)} + Q_{n'}^s, F_n^{(1)}] - D_n^{(1)}[H_n^{(2)} + Q_{n'}^s, F_n^{(2)}]\}. \quad (51)$$

Since the incident field coefficients are known, Eqs. (44) and (45) represent two sets of simultaneous equations which can be solved through matrix inversion techniques for the two sets of field coefficients. Although the solution is general for any incident field, we consider specifically the case of plane wave illumination whose wave vector is oriented at angle α with respect to the z_1 axis as shown in Figure 1. Mie scattering derivations typically restrict the plane wave so that $\alpha = 0$. Since we restrict the nucleus to being centered on the z_1 axis, we must remove the restriction on the incident plane wave for the derivation to be completely general. When the plane wave is polarized perpendicular to the $x-z$ plane (TE), the coefficients are found to be[15]

$$a_{nm} = a_{nm}^{\mathrm{Te}} = \frac{i^n}{n(n+1)}\left[\sqrt{(n-m)(n+m+1)}\,\tilde{P}_n^{m+1}(\cos\alpha) - \sqrt{(n-m+1)(n+m)}\,\tilde{P}_n^{m-1}(\cos\alpha)\right] \quad (52)$$

$$= \frac{2i^{n+2}}{n(n+1)}\frac{\partial}{\partial\alpha}\tilde{P}_n^m(\cos\alpha), \quad (53)$$

$$b_{nm} = b_{nm}^{\mathrm{TE}} = \frac{i^{n+2}(2n+1)}{n(n+1)}\left[\sqrt{\frac{(n-m+1)(n-m+2)}{(2n+1)(2n+3)}}\times\tilde{P}_{n+1}^{m-1}(\cos\alpha) + \sqrt{\frac{(n+m+1)(n+m+2)}{(2n+1)(2n+3)}}\tilde{P}_{n+1}^{m+1}(\cos\alpha)\right] \quad (54)$$

$$= \frac{2i^{n+2}}{n(n+1)}\frac{m\tilde{P}_n^m(\cos\alpha)}{\sin\alpha}. \quad (55)$$

When the plane wave is polarized in the $x-z$ plane (TM), the coefficients are found to be

$$a_{nm} = a_{nm}^{\mathrm{TM}} = ib_{nm}^{\mathrm{TE}} \quad (56)$$

and

$$b_{nm} = b_{nm}^{\mathrm{TM}} = ia_{nm}^{\mathrm{TE}}. \quad (57)$$

2.5 SCATTERING AMPLITUDES AND EFFICIENCIES

We consider the scattering amplitudes in the far field, where $kr_1 \gg ka$. The scattered fields in this case are in the $\hat{\theta}$ and $\hat{\varphi}$ directions. In this limit, the spherical Hankel functions reduce to spherical waves:

$$h_n^{(1)}(kr) \sim \frac{(-i)^n}{ikr}e^{ikr}. \quad (58)$$

The scattering amplitudes can be expressed in the form of the matrix

$$\begin{pmatrix} E_\varphi^{\mathrm{sca}} \\ E_\theta^{\mathrm{sca}} \end{pmatrix} = \frac{e^{ikr_1}}{-ikr_1}\begin{pmatrix} S_1 & S_4 \\ S_3 & S_2 \end{pmatrix}\begin{pmatrix} E_{\mathrm{TE}}^{\mathrm{inc}} \\ E_{\mathrm{TM}}^{\mathrm{inc}} \end{pmatrix}. \quad (59)$$

The scattering amplitude matrix elements are solved by expanding the scattered electric fields [Eq. (4)] in terms of the vector wave functions and then expanding the vector wave functions [Eq. (1)] in terms of the polarization directions. In the far field, the $\hat{r}$ component of the electric field becomes negligible compared with the $\hat{\theta}$ and $\hat{\varphi}$ components. After some algebra, we have the following:

$$S_1 = \sum_{n=0}^{\infty}\sum_{m=-n}^{n}(-i)^n e^{im\varphi_1}\left[d_{nm}^{\mathrm{TE}}\frac{m}{\sin\theta_1}\tilde{P}_n^m(\cos\theta_1) + c_{nm}^{\mathrm{TE}}\frac{\partial}{\partial\theta_1}\tilde{P}_n^m(\cos\theta_1)\right], \quad (60)$$

$$S_2 = -i\sum_{n=0}^{\infty}\sum_{m=-n}^{n}(-i)^n e^{im\varphi_1}\times\left[c_{nm}^{\mathrm{TM}}\frac{m}{\sin\theta_1}\tilde{P}_n^m(\cos\theta_1) + d_{nm}^{\mathrm{TM}}\frac{\partial}{\partial\theta_1}\tilde{P}_n^m(\cos\theta_1)\right], \quad (61)$$

$$S_3 = -i\sum_{n=0}^{\infty}\sum_{m=-n}^{n}(-i)^n e^{im\varphi_1}\times\left[c_{nm}^{\mathrm{TE}}\frac{m}{\sin\theta_1}\tilde{P}_n^m(\cos\theta_1) + d_{nm}^{\mathrm{TE}}\frac{\partial}{\partial\theta_1}\tilde{P}_n^m(\cos\theta_1)\right], \quad (62)$$

$$S_4 = \sum_{n=0}^{\infty}\sum_{m=-n}^{n}(-i)^n e^{im\varphi_1}\left[d_{nm}^{\mathrm{TM}}\frac{m}{\sin\theta_1}\tilde{P}_n^m(\cos\theta_1) + c_{nm}^{\mathrm{TM}}\frac{\partial}{\partial\theta_1}\tilde{P}_n^m(\cos\theta_1)\right]. \quad (63)$$

Using the following relationship for normalized, associated Legendre polynomials

$$\tilde{P}_n^{-m}(\cos\theta_1) = (-1)^m\tilde{P}_n^m(\cos\theta_1) \quad (64)$$

the following relationships between the scattering coefficients may be derived

$$c_{n\bar{m}}^{\mathrm{TE}}=(-1)^m c_{nm}^{\mathrm{TE}},$$
$$c_{n\bar{m}}^{\mathrm{TM}}=(-1)^{m+1} c_{nm}^{\mathrm{TM}},$$
$$d_{n\bar{m}}^{\mathrm{TE}}=(-1)^{m+1} d_{nm}^{\mathrm{TE}},$$
$$d_{n\bar{m}}^{\mathrm{TM}}=(-1)^m d_{nm}^{\mathrm{TM}}, \tag{65}$$

where $\bar{m}=-m$.

The scattering, extinction, and absorption efficiencies of the system are defined as the cross sections per projected area and may be expressed as

$$Q_{\mathrm{sca}}=\frac{2}{(ka_1)^2}\left[\sum_{n=1}^{\infty} n(n+1)\sum_{m=-n}^{n}(|c_{nm}^{\mathrm{TE}}|^2+|d_{nm}^{\mathrm{TE}}|^2 + |c_{nm}^{\mathrm{TM}}|^2+|d_{nm}^{\mathrm{TM}}|^2)\right], \tag{66}$$

$$Q_{\mathrm{ext}}=\frac{-2}{(ka_1)^2}\mathrm{Re}\left[\sum_{n=1}^{\infty} n(n+1)\sum_{m=-n}^{n}(c_{nm}^{\mathrm{TE}}a_{nm}^{\mathrm{TE}*} + d_{nm}^{\mathrm{TE}}b_{nm}^{\mathrm{TE}*}+c_{nm}^{\mathrm{TM}}a_{nm}^{\mathrm{TM}*}+d_{nm}^{\mathrm{TM}}b_{nm}^{\mathrm{TM}*})\right], \tag{67}$$

$$Q_{\mathrm{abs}}=Q_{\mathrm{ext}}-Q_{\mathrm{sca}}, \tag{68}$$

where a_{nm}^{*} and b_{nm}^{*} are the complex conjugates of a_{nm} and b_{nm}, respectively. The asymmetry parameter g is a measure of radiation pressure on the system and is a necessary parameter used in cell levitation. This quantity can be expressed as

$$g=\frac{4}{Q_{\mathrm{sca}}(ka)^2}\sum_{n,m} m\ \mathrm{Re}(c_{nm}^{\mathrm{TE}}d_{nm}^{\mathrm{TE}*}+c_{nm}^{\mathrm{TM}}d_{nm}^{\mathrm{TM}*})+n(n+2)\sqrt{\frac{(n-m+1)(n+m+1)}{(2n+3)(2n+1)}}\,\mathrm{Re}[i(c_{nm}^{\mathrm{TE}}c_{n+1m}^{\mathrm{TE}*} + d_{nm}^{\mathrm{TE}}d_{n+1m}^{\mathrm{TE}*}+c_{nm}^{\mathrm{TM}}c_{n+1m}^{\mathrm{TM}*}+d_{nm}^{\mathrm{TM}}d_{n+1m}^{\mathrm{TM}*}]. \tag{69}$$

Detailed derivations for the asymmetry parameter and the efficiencies are given elsewhere.[19]

3 RESULTS

Although Eqs. (60)–(63) describe the electromagnetic field scattered by the cell, the meat of the problem is solving the simultaneous equations described by Eqs. (44) and (45). For practical purposes, only a finite number N of vector spherical harmonics are necessary to describe the scatter from this system. In our calculations we use the criterion developed by Wiscombe[20] and Bohren and Huffman[18] that $N=x+4x^{1/3}+2$ where $x=2\pi a_3/\lambda$. Higher order terms are insignificant and their corresponding coefficients can safely be set to zero. We are left with solving $2N$ simultaneous equations. Solving this resulting matrix is an N^3 process, so for large-size parameters the computation time slows down dramatically. For example, the CPU time required to calculate the scatter (1° scattering resolution in a plane) for an $x=25$ cell is approximately 28 s on a SUN 4 workstation and is approximately 175 s for an $x=50$ cell.

We demonstrate one application of the model by calculating the light-scattering Mueller matrix elements having slightly different system parameters. These matrix elements are shown for cells having different cell-membrane refractive indices (chemistry) in Figure 2. The structure of the total intensity (element S_{11}) of the scattered light is essentially the same for all three systems. The position of the maxima and minima are virtually the same, but the amplitudes of the maxima tend to increase (especially in the backscatter region) as the cell-membrane refractive index is increased. The polarization Mueller matrix elements (matrix elements S_{12}, S_{33}, and S_{34} are shown) show a marked difference. The position of the maxima and minima remain virtually unchanged in the forward-scatter region, but in the backscatter these minima and maxima shift, and the amplitudes are significantly different. These results are consistent with previous experimental studies which found the backscatter region of the polarization matrix elements to be extremely sensitive to small system changes.[5–8] Finally, it should be noted that the cell parameters of this figure are not realistic: the sizes are too small and the refractive indices are too large. The particular parameters were chosen to illustrate the scattering effects seen. These same effects can also be seen in the scatter from cells having more realistic parameters, but due to the higher frequency oscillations in the scattering signals (oscillation frequency increases with particle size), it is much more difficult to see any trends in the data, so these were chosen for illustrative purposes.

Figure 3 shows the light-scattering Mueller matrix elements for cells having different nucleus positions. These results look similar to the previous results. Although the total intensity varies more than for the cell-membrane study, the polarization matrix elements still display greater sensitivity, and the backscattered light is most sensitive to changes in the system geometry.

From Figures 2 and 3, it is apparent that the backscatter is the most sensitive region to small changes in the particle geometry and chemistry. We now examine just the backscatter from a larger, more realistic cell. The system parameters are chosen to correspond to a 10 μm cell contained in an aqueous external media ($m=1.33$) illuminated in the near-infrared ($\lambda=850$ nm), and are similar to values used in other models.[3,11,13] Figure 4 shows the backscatter Mueller matrix for three different cytoplasm chemistries. Even though the cytoplasm refractive index change is only 1% between runs, the backscatter signals change significantly. The maximum

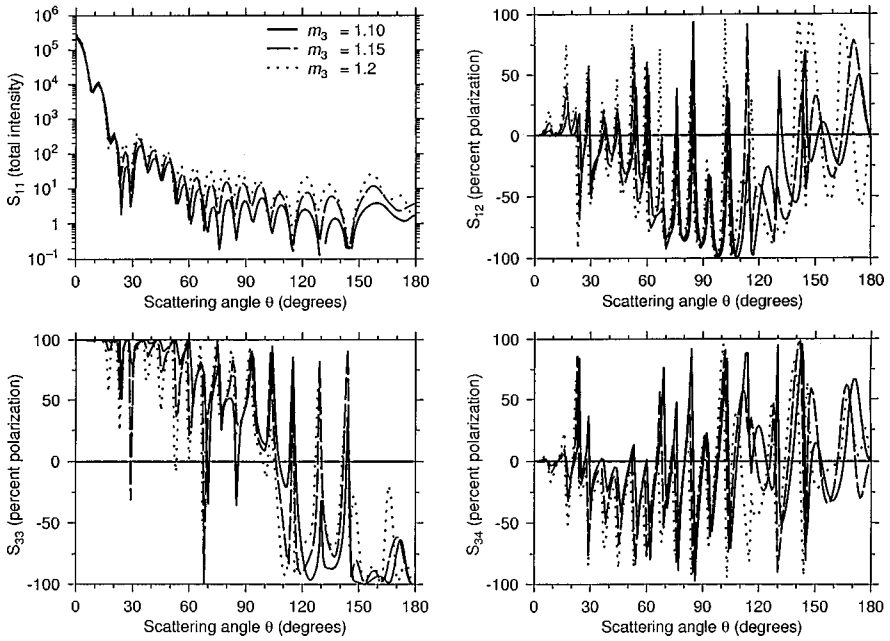

Fig. 2 Light scattering Mueller matrix elements as a function of scattering angle at three different cell membrane refractive indices. For this system, $\lambda = 0.6328\ \mu m$, $a_1 = 2.4\ \mu m$, $a_2 = 1.0\ \mu m$, $a_3 = 2.5\ \mu m$, $m_1 = 1.05$, $m_2 = 1.15$, $d = 1.0\ \mu m$.

oscillation frequency which is determined primarily by the size of the cell remains constant between runs, but the positions of the maxima and minima are shifted in not only the polarization matrix elements, but in the total intensity matrix element S_{11} as well. The 50% differences in the percent polarization signals are not uncommon.

4 CONCLUSION

We have derived solutions for the total field when an incident plane wave strikes a cellular system. Because of the nature of the solution, numerical results can be calculated quite rapidly compared to other techniques. The derivation places no restric-

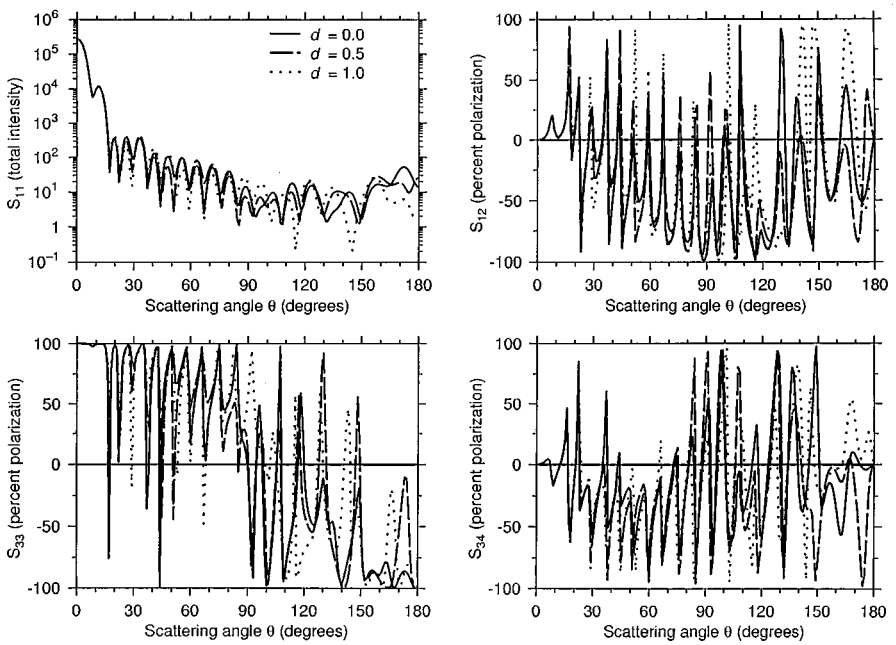

Fig. 3 Light scattering Mueller matrix elements as a function of scattering angle at three different cell nucleus locations. For this system, $\lambda = 0.6328\ \mu m$, $a_1 = 2.4\ \mu m$, $a_2 = 1.0\ \mu m$, $a_3 = 2.5\ \mu m$, $m_1 = 1.05$, $m_2 = 1.15$, $m_3 = 1.20$.

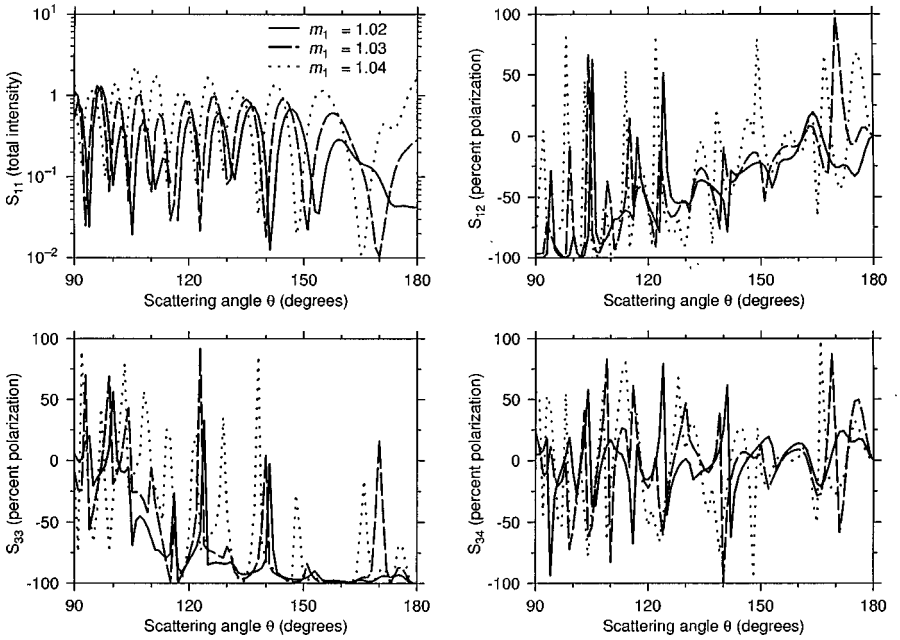

Fig. 4 Light scattering Mueller matrix elements as a function of scattering angle for three different cytoplasm chemistries. For this system, $\lambda = 0.639\ \mu m$, $a_1 = 4.99\ \mu m$, $a_2 = 2.0\ \mu m$, $a_3 = 5.0\ \mu m$, $m_2 = 1.05$, $m_3 = 1.1$, and $d = 1.0\ \mu m$.

tions on the refractive indices of the particle constituents or the size of the system; however, computation times increase with cell size. The model may be used to examine the scattering sensitivity to geometrical and chemical changes of the cell. For more complicated cellular systems containing additional irregularities, it might be possible to calculate scattering and absorption efficiencies by incorporating effective medium approximations into the model. It may also be used to calculate the scatter from a fluorescing molecule located at some position within the cell. In our simulations of the light scattering Mueller matrix, we find that the backscatter is extremely sensitive to small changes in the system parameters. We demonstrate that even a very small ($\sim 1\%$) change in system parameters can have a drastic effect on the scattered light. Since it is extremely difficult to characterize cells to such an extent due to geometrical, orientational, and chemical changes in time, for many modeling simulations it is necessary to calculate average scattering properties. Such calculations are computationally expensive. This manuscript provides a technique which can greatly facilitate such calculations.

APPENDIX A: TRANSLATION ADDITION OF SPHERICAL HARMONICS

Stein[23] and Cruzan[24] derived translation addition theorems for vector spherical wave functions. For a translation along the z axis with no rotation, the vector spherical harmonics are related by

$$M_{nm,2}^{(q)} = \sum_{n'=0}^{\infty} A_{n'}^{(n,m,q)} M_{n',m,1}^{(q)} + B_{n'}^{(n,m,q)} N_{n'm,1}^{(q)}, \tag{A1}$$

$$N_{nm,2}^{(q)} = \sum_{n'=0}^{\infty} B_{n'}^{(n,m,q)} M_{n'm,1}^{(q)} + A_{n'}^{(n,m,q)} N_{n'm,1}^{(q)}, \tag{A2}$$

where q denotes the order of the spherical Bessel functions ($q = 3, 4$). This relationship is valid in the region where $r > |d|$. The translation coefficients $A_{n'}^{(n,m,q)}$ and $B_{n'}^{(n,m,q)}$ can be calculated from the scalar translation coefficients, $C_{n'}^{(n,m,q)}$:

$$A_{n'}^{(n,m,q)} = C_{n'}^{(n,m,q)} - \frac{k_1 d}{n'+1}\sqrt{\frac{(n'-m+1)(n'+m+1)}{(2n'+1)(2n'+3)}}\, C_{n'+1}^{(n,m,q)} - \frac{k_1 d}{n'}\sqrt{\frac{(n'-m)(n'+m)}{(2n'+1)(2n'-1)}}\, C_{n'-1}^{(n,m,q)}, \tag{A3}$$

$$B_{n'}^{(n,m,q)} = \frac{-ik_1 md}{n'(n'+1)}\, C_{n'}^{(n,m,q)}. \tag{A4}$$

The $C_{n'}^{(n,m,q)}$ are scalar translation coefficients. These can be found via recursion relations:[21]

$$C_{n'}^{(0,0,q)} = \sqrt{2n'+1}\, j_{n'}(k_1 d), \tag{A5}$$

$$C_{n'}^{(-1,0,q)} = -\sqrt{2n'+1}\, j_{n'}(k_1 d), \tag{A6}$$

$$C_{n'}^{(n+1,0,q)}=\frac{1}{(n+1)}\sqrt{\frac{2n+3}{2n'+1}}\left\{n'\sqrt{\frac{2n+1}{2n'-1}}\,C_{n'-1}^{(n,0,q)}+n\sqrt{\frac{2n'+1}{2n-1}}\,C_{n'}^{(n-1,0,q)}-(n'+1)\sqrt{\frac{2n+1}{2n'+3}}\,C_{n'+1}^{(n,0,q)}\right\}, \tag{A7}$$

$$\sqrt{(n-m+1)(n+m)(2n'+1)}C_{n'}^{(n,m,q)}=\sqrt{(n'-m+1)(n'+m)(2n'+1)}C_{n'}^{(n,m-1,q)}-k_1 d\sqrt{\frac{(n'-m+2)(n'-m+1)}{(2n'+3)}}\,C_{n'+1}^{(n,m-1,q)}-k_1 d\sqrt{\frac{(n'+m)(n'+m-1)}{2n'-1}}\,C_{n'-1}^{(n,m-1,q)}, \tag{A8}$$

and

$$C_{n'}^{(n,m,q)}=C_{n'}^{(n,-m,q)}. \tag{A9}$$

From these equations, we see that

$$A_{n'}^{(n,m,3)}=A_{n'}^{(n,m,4)}=A_{n'}^{(n,-m,3)}=A_{n'}^{(n,m)}, \tag{A10}$$

$$B_{n'}^{(n,m,3)}=B_{n'}^{(n,m,4)}=B_{n'}^{(n,-m,3)}=B_{n'}^{(n,m)}, \tag{A11}$$

$$C_{n'}^{(n,m,3)}=C_{n'}^{(n,m,4)}=C_{n'}^{(n,-m,3)}=C_{n'}^{(n,m)}. \tag{A12}$$

REFERENCES

1. P. J. Wyatt, ''Identification of bacteria by differential light scattering,'' *Nature* **221**, 1257–1258 (1969).
2. A. L. Koch and E. Ehrenfeld, ''The size and shape of bacteria by light scattering measurements,'' *Biochim. Biophys. Acta* **165**, 262–273 (1968).
3. A. Brunsting and P. Mullaney, ''Differential light scattering from spherical mammalian cells,'' *Biophys. J.* **14**, 439–453 (1974).
4. R. Meyer, ''Light scattering from biological cells: dependence of backscatter radiation on membrane thickness and refractive index,'' *Appl. Opt.* **18**, 585–588 (1979).
5. W. S. Bickel, J. F. Davidson, D. R. Huffman, and D. R. Kilkson, ''Application of polarization effects in light scattering: A new biophysical tool,'' *Proc. Natl. Acad. Sci. USA* **73**, 486–490 (1976).
6. R. G. Johnston, S. B. Singham, and G. C. Salzman, ''Polarized light scattering,'' *Comm. Molec. Cell Biophys.* **5**, 171–202 (1988).
7. W. P. van de Merwe, B. V. Bronk, and D. R. Huffman, ''Reproducibility and sensitivity of polarized light scattering for identifying bacterial suspensions,'' *Appl. Opt.* **28**, 5052–5057 (1990).
8. B. V. Bronk, W. P. van de Merwe, and M. Stanley, ''*In vivo* measure of average bacterial cell size from a polarized light scattering function,'' *Cytometry* **13**, 155–162 (1992).
9. G. J Streekstra, A. G. Hoekstra, E. J. Nijhof, and R. M. Heethaar, ''Light scattering by red blood cells in ektacytometry: Fraunhofer versus anomalous diffraction,'' *Appl. Opt.* **32**, 2266–2272 (1993).
10. G. J Streekstra, A. G. Hoekstra, and R. M. Heethaar, ''Anomalous diffraction by arbitrarily oriented ellipsoids: Applications in ektacytometry,'' *Appl. Opt.* **33**, 7288–7296 (1994).
11. J. Maier, S. Walker, S. Fantini, M. Franceschini, and E. Gratton, ''Possible correlation between blood glucose concentration and the reduced scattering coefficient of tissues in the near infrared,'' *Opt. Lett.* **19**, 2062–2064 (1994).
12. A. Dunn, C. Smithpeter, A. J. Welch, and R. Richards-Kortum, ''Light scattering from cells,'' in *Biomedical Optical Spectroscopy and Diagnostics, 1996 Technical Digest*, Optical Society of America, Washington DC, pp. 50–52 (1996).
13. A. Dunn and R. Richards-Kortum, ''Three-dimensional computation of light scattering from cells,'' *IEEE J. Sel. Topics Quantum Electron.* **2**, 898–905 (1996).
14. D. Ngo, G. Videen, and P. Chýlek, ''A FORTRAN code for the scattering of EM waves by a sphere with a nonconcentric spherical inclusion,'' *Comp. Phys. Comm.* **1077**, 94–112 (1996).
15. G. Videen, D. Ngo, P. Chýlek, and R. G. Pinnick, ''Light scattering from a sphere with an irregular inclusion,'' *J. Opt. Soc. Am. A* **12**, 922–928.
16. S. C. Hill, G. Videen, and J. D. Pendleton, ''Reciprocity method for obtaining the far fields generated by a source inside or near a microparticle,'' *J. Opt. Soc. Am. B* **14**, 2522–2529 (1997).
17. M. Abramowitz and I. A. Stegun, Eds., *Handbook of Mathematical Functions*, Dover, New York (1972).
18. C. F. Bohren and D. R. Huffman, *Absorption and Scattering of Light by Small Particles*, Wiley, New York (1983).
19. D. Ngo, Light scattering from a sphere with a nonconcentric spherical inclusion, Ph.D. dissertation, Department of Physics, New Mexico State University, Las Cruces, 1994.
20. W. J. Wiscombe, ''Improved Mie scattering algorithms,'' *Appl. Opt.* **19**, 1505–1509 (1980).
21. P. Chýlek, V. Srivastava, R. G. Pinnick, and R. T. Wang, ''Scattering of electromagnetic waves by composite spherical particles: Experiment and effective medium approximations,'' *Appl. Opt.* **27**, 2396–2404 (1988).
22. G. Videen, D. Ngo, and P. Chýlek, ''Effective-medium predictions of absorption by graphitic carbon in water droplets,'' *Opt. Lett.* **19**, 1675–1677 (1994).
23. S. Stein, ''Addition theorems for spherical wave functions,'' *Quart. Appl. Math.* **19**, 15–24 (1961).
24. O. R. Cruzan, ''Translational addition theorems for spherical vector wave functions,'' *Quart. Appl. Math.* **20**, 33–40 (1962).